A study of coating water loss and immobilization under dynamic conditions

Teng Shau Young, Donald E. Pivonka, Lois G. Weyer, and Bob Ching

ABSTRACT: Gloss decay and immobilization solids data show that water retention on a short-dwell-type coater depends on the coating water viscosity and the capability of the coating to form a high solids cake barrier at the coating and paper interface. Clay–adsorbing thickeners give a higher degree of solids flocculation and lower immobilization solids as well as better coverage, smoothness, and rotogravure printability than thickeners with low clay affinity.

KEYWORDS: Blade coaters, coating, computers, gloss meters, immobilization, moisture, on line measurement, retention, thickeners, water, water removal.

Coating water loss is one of the most critical concerns in coated paper production and has been the subject of numerous studies *(1–19)*. It is of specific importance in blade coating operations where excessive water loss to the basestock may cause runnability or quality defects. These defects include scratching, blade bleeding, streaking caused by undesired rheology and solids buildup, web break from weakening of the basestock, surface roughening due to fiber swelling, and print mottle *(15)*. Consequently, water retention or the prevention of excessive water loss is of keen interest to blade coating practitioners.

This work primarily concerns water loss and the associated immobilization phenomena in high-speed coating processes involving a short dwell time blade coater. **Figure 1** shows such a process. A low pressure applicator deposits the coating shortly before it encounters the blade. When traveling under the blade, the coating experiences a large hydrodynamic pressure for a short duration, e.g., approximately 10^{-5} s for a 0.38 mm (0.015 in.) thick blade at a 50° angle and a speed of 1220 m/min (4000 ft/min). The coating under pressure tends to move as a "plug flow" into the porous basestock. It likely will first penetrate the larger pores, such as "pin holes." Then it will penetrate the tighter porous paper medium. Conceivably, water and some binders will migrate into the paper medium while the bulk of the pigments and other solids remain on the surface. A high solids filter cake may eventually form near the interface. This progressively grows in thickness as the coating continues to lose water *(9)*. Meanwhile, capillary migration *(3-5)* occurs after the coating water wets the paper until the coating consolidates in the dryer. The extent of water loss in such a process may vary widely with coating formulation, basestock, and sometimes machine setting.

In this work, our specific interest is in water loss control through coating formulating. We assume that we cannot control the machine conditions or the formation, sizing, and temperature of the basestock. The literature addresses several possible approaches in this regard *(1, 2, 9, 14, 17, 18)*.

According to the Washburn equation *(17)*, increasing the water viscosity with addition of a water soluble polymeric thickener or co–binder may slow the capillary migration. Sometimes a change in the binder surfactant also will reduce paper wetting *(18)*. In the case of pressure migration before cake formation, one or a combination of the following may conceivably reduce water loss:

- Reducing the driving force and blade pressure
- Increasing the water viscosity by adding a thickener or co–binder
- Increasing the coating solids to reduce available water and flow pathway

Young is research scientist, Pivonka is senior research scientist, and Weyer is senior research scientist with Hercules Inc., Wilmington, DE 19894. Ching is research engineer at Engelhard Corp., Menlo Park, Edison, NJ 08818.

1. Coating dewatering under blade

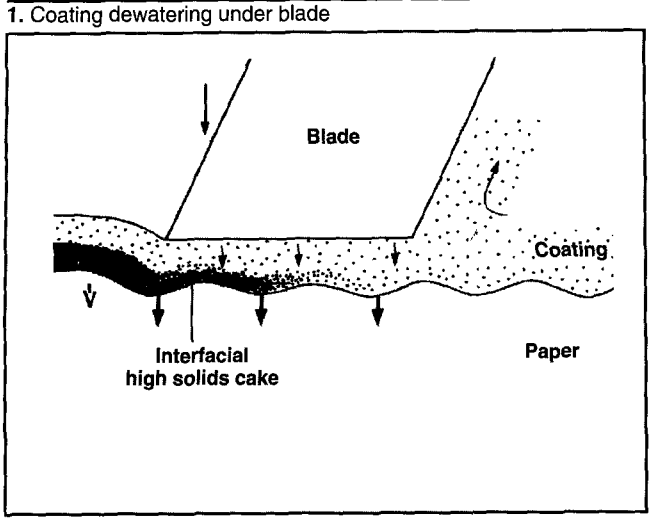

2. CLC coater test diagram

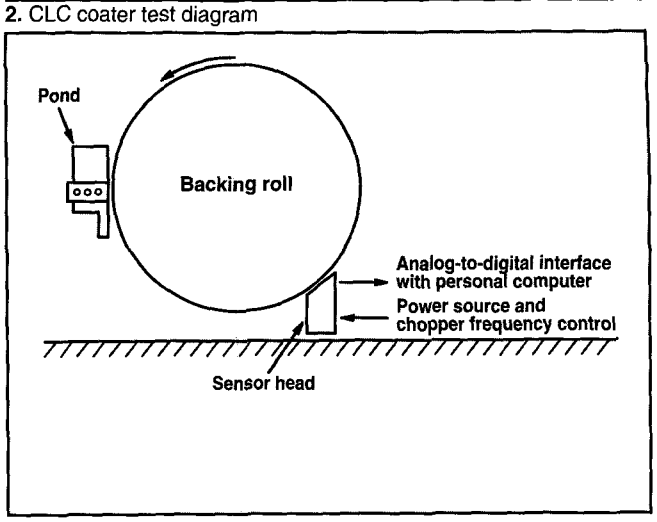

- Using platey pigments which tend to pack closely in a direction parallel to the flow field under the blade causing added tortuosity to resist the passage of fluid under pressure *(14)*.

After the formation of the cake, the flowing water has to move through an additional porous medium which has much smaller pore openings than the paper medium. Pressure migration through such a filter cake follows a Hagen–Poiseulle type equation *(9, 12)*. This predicts a sharp flow reduction with decreased pore opening to the fourth power. Cake formation should therefore substantially reduce subsequent water migration. Other investigators have discussed the importance of cake formation *(7, 9, 10)*. This has received some experimental support from pilot coater studies *(7, 10)*.

Many of the above approaches are mutually exclusive or difficult to implement because of rheological or other problems. Among all known approaches, raising the water viscosity with a thickener or co–binder such as carboxymethylcellulose, polyacrylate emulsion, or starch is the most common practice today. These polymeric thickeners or co–binders, however, can have a much greater role than water and coating thickening. Some polymeric thickeners undergo association with clays to cause structure building and faster coating immobilization *(20, 21)*. As a result, they may also alter the cake formation behavior of the coating during high-speed coating. One of our objectives was to understand how thickener and clay interactions could influence cake formation and therefore water retention.

We undertook a laboratory study to learn the effect of thickener and clay interaction on cake formation and water retention under high-speed coating conditions. This study involved two major efforts. One concerned the detection of coating water loss and immobilization on a high-speed laboratory coater. The other was an effort to provide background information for the high-speed coater study. It involved measurements of thickener and clay interaction, coating structure and rheology, immobilization behavior, and water loss behavior under conditions of low pressure and low speed.

Our first effort required the development of a new method for the measurement of moisture-related properties under high-speed, high-pressure conditions. We developed a method which involved the use of a rapid response, noncontact light reflection detector to monitor coating gloss changes on a CLC laboratory coater. We later related the on–coater gloss change to surface moisture by simultaneously measuring the coating gloss and moisture on a nonporous plate. This developmental work was necessary because all the known laboratory water retention measurements can only operate under conditions of low speeds and pressure. Under these conditions, the cake formation process may not be properly simulated.

I. Adsorption of polymers on clay and paper fiber

Polymer	*Chemical nature*	*Clay*	*Paper*
A	Anionic, acrylate–based	Not detected	Not detected
B	Anionic, cellulosic	0.06	14.5
C	Nonionic, cellulosic	0.22	25.5
D	Nonionic, cellulosic self–associative	0.23	14.4

We used the noncontact reflection detector to evaluate a series of rotogravure light weight coated (LWC) coatings that had distinct coating rheology and immobilization behavior. These differences in coating properties occurred as a result of the use of four different polymeric thickeners that had different clay affinities. Later sections of this paper report the observed coating properties, on–coater gloss decay behavior, and optical and rotogravure printing properties of the

3. Gloss decay curve observed on bench–top coater

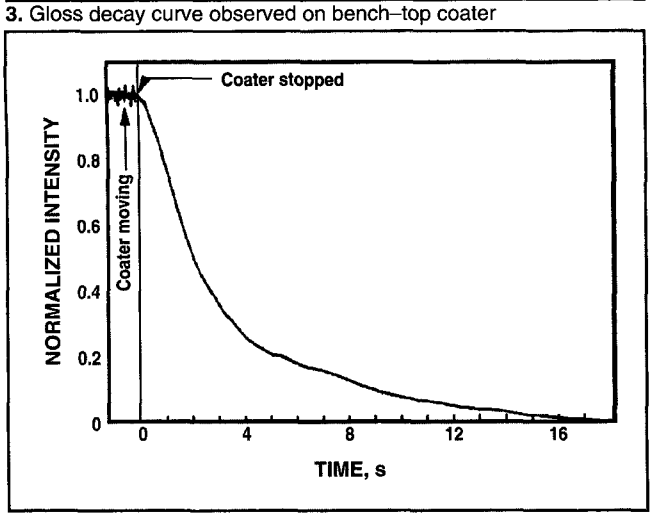

4. Diagram SGM measurement

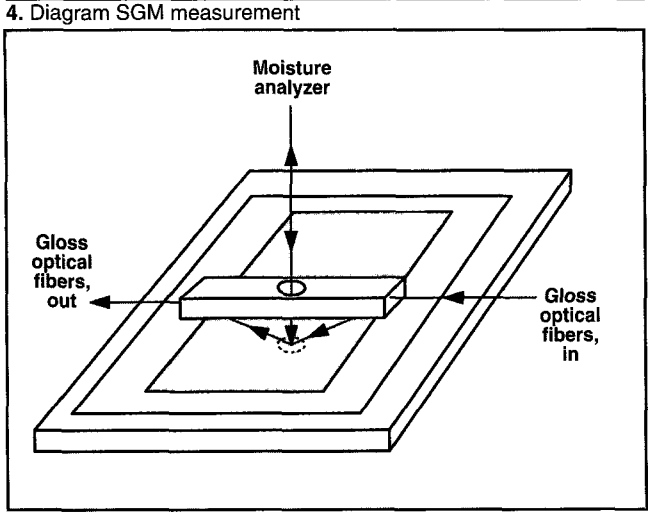

coated papers and discuss their characteristics relating to coating structure and rheology.

Coating materials and testings

This study used a rotogravure formulation comprising 50 parts U.S. delaminated clay, 50 parts U.S. No. 2 clay, 7 parts styrene butadiene latex, 1 part calcium stearate, and a varying amount of thickener. We tested the coatings at 55% and 60% solids levels. Sodium hydroxide additions controlled the pH of the coatings to a range of 8.0 to 8.5. Addition of thickener adjusted all test coatings to the same Brookfield viscosity of 1000 mPa·s (cp) at 100 rpm.

The study used four polymeric thickeners of varying degrees of clay affinity to demonstrate the effect of clay association on coating structure, cake forming tendency, and water migration. **Table I** describes the nature and relevant properties of these four polymers. The designation under clay is the adsorption on No. 1 clay in mg of polymer per m^2 of clay at an initial polymer concentration of 0.4 parts of polymer per 100 parts of clay. The designation under paper is the weight percentage of polymer adsorbed on paper fibers.

Polymer A was a low viscosity type alkali–swellable polyacrylate emulsion which did not adsorb on U.S. clays *(21)*. Polymers B, C, and D were cellulose derivatives that had the same nominal mol. wt. of ca. 300,000. Polymer B was a sodium carboxymethylcellulose which had a low degree of clay adsorption. Polymer C was a nonionic, hydroxyethylcellulose–based derivative which adsorbed on clays strongly. Polymer D, like Polymer C, was also nonionic and clay–adsorbing. It had a further chemical modification so that the polymer molecules could associate with one another in an aqueous medium through hydrophobe to hydrophobe association *(21)*.

We tested each of the coatings for water loss pattern using the noncontact reflection method on a CLC laboratory coater. We also tested two coating samples for surface reflection changes on a bench–top coater. We characterized all coatings for high shear viscosity, water retention time, viscoelasticity, and after–shear structure recovery.

We supercalendered the paper samples from the CLC coater through 3 nips at 74°C and 45 kN/m before evaluation of 75° gloss, opacity, brightness, smoothness, and rotogravure printability. We measured the coating smoothness and rotogravure printability using Parker Print–Surf (PPS) and IGT Heliotest, respectively.

Method development

On–line coating gloss measurement on laboratory coater

We built a noncontact on–line gloss measuring device capable of monitoring rapid gloss changes during blade coating. It consisted of the following components:

- Optical fibers which direct the source radiation from a 12V dc tungsten light toward the paper surface at a 75° incident angle
- A frequency chopper which modulates the frequency of the incident light
- A detector, preamplifier, and lock–in amplifier system which detects the optical fiber–guided reflected light
- An analog–to–digital converter which connects to a personal computer for data acquisition.

The instrument measured the surface light reflection at a distance of 1 cm from the paper. By modulating the frequency of the incident and reflected light, there was virtual elimination of the interference of stray light.

Using this noncontact detector with a Model 6000 CLC laboratory coater allowed study of coating gloss changes during high-speed blade coating. In this study, the on–line gloss measuring device had a position under the

5. Near–IR spectra of a drying coating

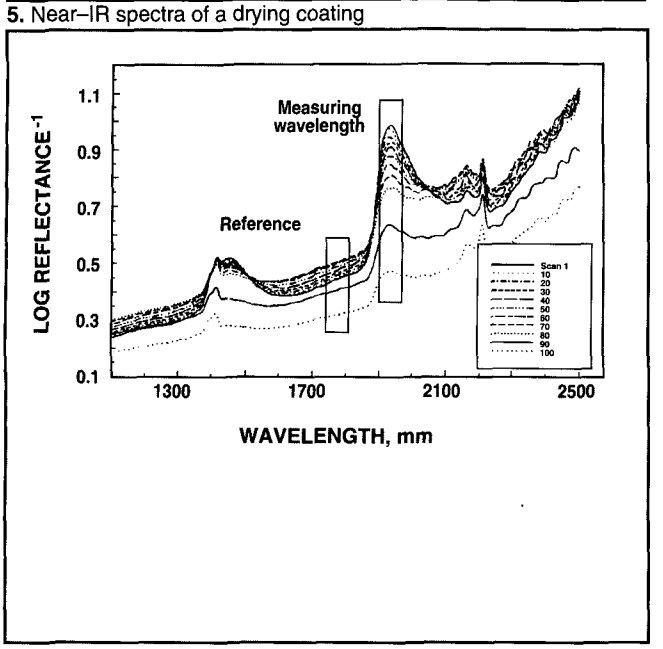

6. Calibration curve for near–IR detector

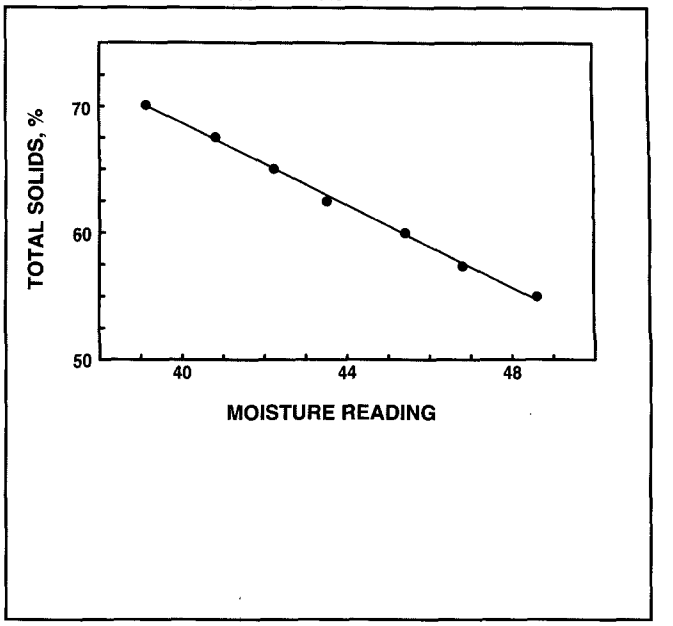

coater depicted in **Fig. 2**. To avoid any physical contact with the moving parts of the CLC coater, the location of the sensor head of the device was at a point about 0.92 m (3 ft) away from the blade. At a coating speed of 1220 m/min, this translated into a delay time of about 45 ms after blade metering. Note that modification of the CLC coater configuration will largely reduce this distance.

In CLC tests, we applied coating to the wire side of a commercial 36 g/m^2 LWC basestock at 915 and 1220 m/min (3000 and 4000 fpm) using a 0.38-mm-thick blade at a 50° angle. Infrared (IR) drying preconditioned the paper at a 60% intensity. Micrometer adjustment provided coat weight control at 5.0 lb/3300 ft^2 (7.4 g/m^2). The on–line gloss detector monitored the gloss of the paper over a 25-s span at a rate of 100 measurements per s. In one series of tests, IR post–drying at 100% intensity started after the paper had traveled 5 m from the blade. In another two series of tests, the post–drying commenced after 50 m so that the observed gloss decay was due primarily to water penetration into the basestock.

There was also a limited amount of work on a bench–top coater. In this case, the sensor head was about 1 in.

7. Coating immobilization curves from five repeated SGM measurements

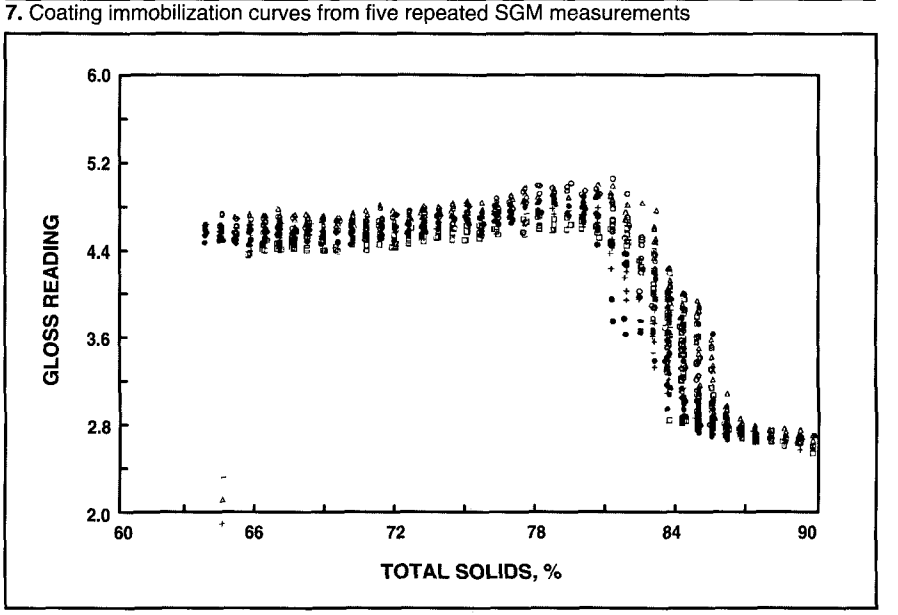

after the blade. With the detector on, the paper web traveling at a speed of 40 ft/min stopped immediately after blade metering. **Figure 3** shows a typical gloss decay curve.

Simultaneous measurement of coating gloss and moisture

To relate on–coater gloss changes to coating solids and immobilization behavior, we conducted a study of coating gloss decay behavior on a nonporous glass plate. In this study, we monitored the gloss and moisture content of the coating simultaneously using the on–line gloss device and a commercial noncontact moisture meter. The sensor heads of the two meters had a location so that both aimed at the same coated area as **Fig. 4** indicates. This arrangement essentially eliminated any sampling errors due to surface and coating weight nonuniformity.

8. Stress relaxation curves for 60% solids coatings

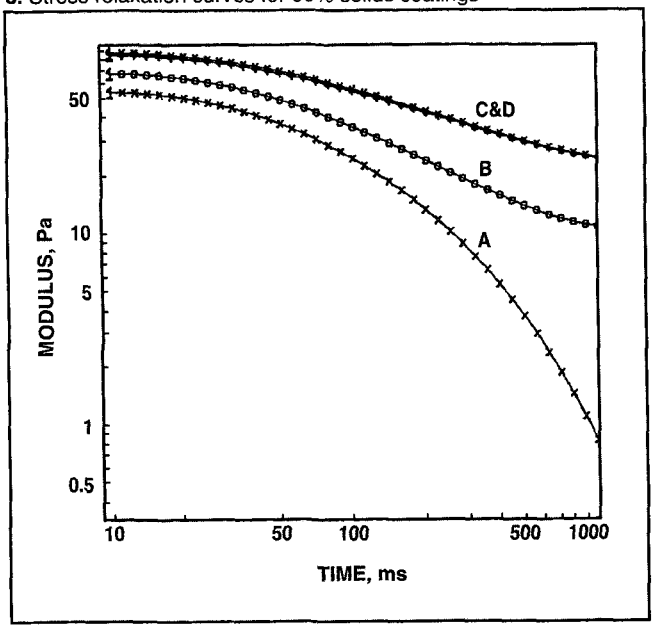

9. Stress relaxation curves for 55% solids coatings

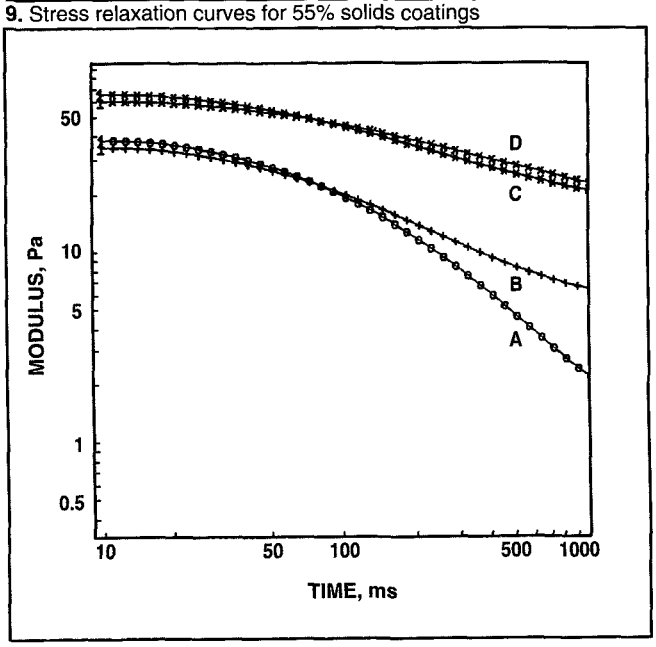

II. Properties of test coatings

Polymer	Concentration, parts	Hercules viscosity, cp	Water retention time, s	Liquid viscosity
60% solids				
A	0.67	52.7	20	16.8
B	0.49	46.5	16	12.1
C	0.42	92.4	10	2.0
D	0.36	47.2	7	1.4
55% solids				
A	1.36	46.2	23	-
B	0.95	34.0	19	-
C	0.73	61.1	13	-
D	0.55	38.5	8	-

The meter detects sample moisture by near–IR absorption of molecular water. **Figure 5** is an example of near–IR spectra of a drying coating sample in which the water absorption bands show progressively lower absorption with time. After laborious calibration studies, we selected an operating wavelength of 1940 nm for the detection of coating water content. At this wavelength, the interference due to clay absorption appears to be minimal and the calibration curve is virtually linear as **Fig. 6** shows.

The moisture reading relates to coating solids by Eq. 1:

$$\text{Solids} = 132 - 1.6(\text{moisture reading}) \quad (1)$$

The equation has a correlation coefficient of 0.998. Note that this calibration applied only to coatings with a solids level below gloss immobilization solids (GIMS). The water absorption intensity dropped abruptly when the dried sample had a solids level above GIMS as Fig. 5 shows. This reflects sudden changes in the structure of the coating and its light-scattering behavior. One limitation of the near–IR technique was the relatively long response time of 0.5 s in this work. While this response time was fast enough to monitor moisture changes in drawdown tests, it was not sufficient to capture the rapid changes on a high-speed coater such as the CLC.

When studying the coating gloss decay and immobilization behavior using the simultaneous gloss and moisture (SGM) measurement, we applied the coating onto a glass plate placed on top of a PTFE block using a 2-mil drawdown frame. Immediately after making the drawdown, we placed the glass plate under the detection heads of Fig. 4 and triggered the computer data acquisition. We monitored the gloss and moisture changes due to air drying for 480 s. This was long enough to cover the consolidation processes. All coating samples showed uniform drying as indicated by uniform surface gloss changes throughout the measurement.

The SGM method was a very efficient way to measure coating immobilization solids. It provided a record of gloss and moisture changes during the entire coating consolidation process in only a few minutes. With a constant sampling area and computer data acquisition, the SGM measurement is less prone to sampling and operator errors and therefore more reproducible than conventional immobilization solids methods. Plots shown in **Fig. 7** for coating gloss vs. moisture reading for five repetitive measurements indicate that the immobilization behavior appears quite reproducible despite some noise from the measuring environment.

Coating properties

Coating structure and rheology

Table II shows the large differences in coating properties which result from

10. Gloss and moisture readings as functions of time during consolidation

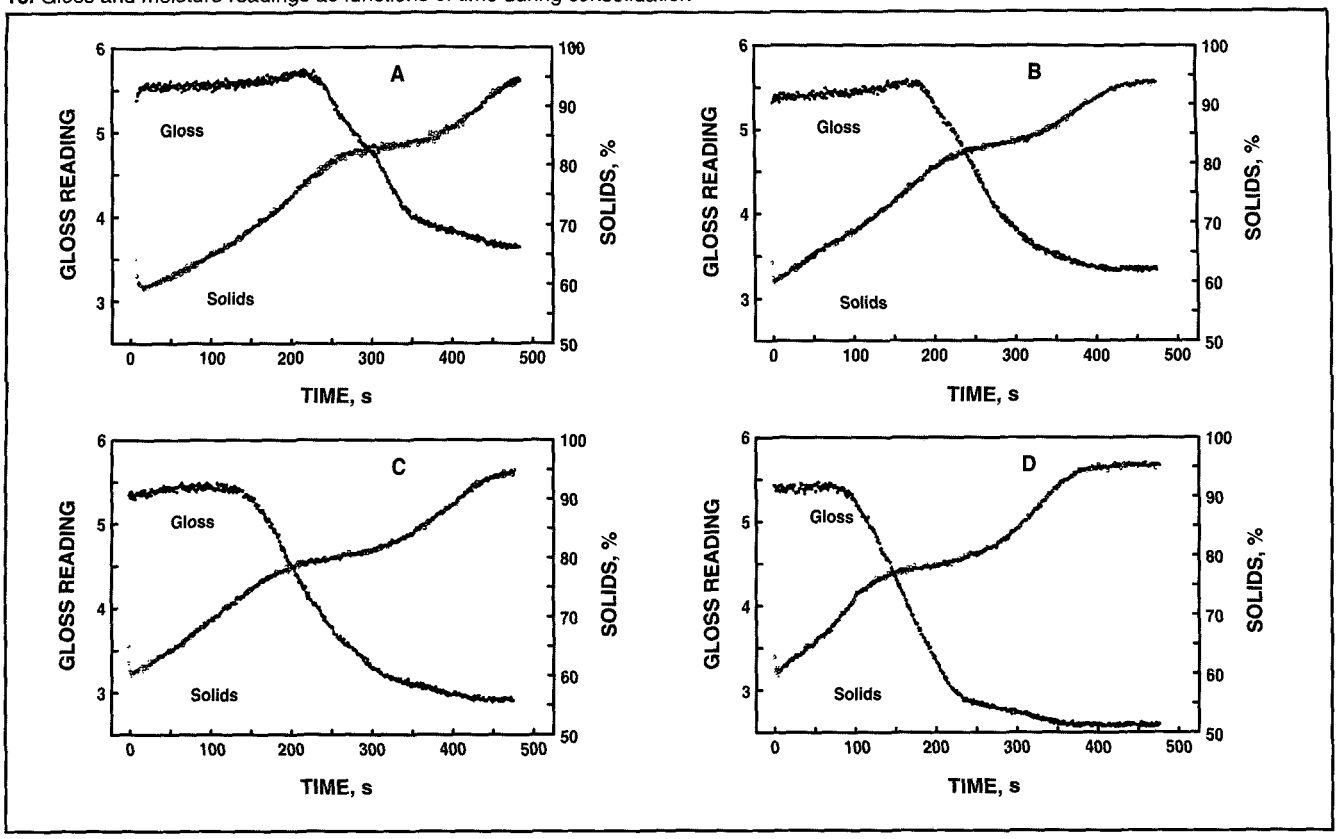

the addition of thickeners having different clay affinities to the rotogravure coating. In this table, we measured the liquid viscosity at 105 s^{-1} on a rheometer with parallel plate geometry. We isolated the coating liquid by centrifuging it twice at 30,000 g. The thickener dosage requirement was the highest for Polymer A, which was a nonadsorbing (to clay), low-viscosity type polyacrylate. The high dosage and nonadsorbing nature led to a high coating water viscosity and a long water retention time measured under static, no pressure conditions. The three cellulosic thickeners, B, C, and D, were of higher molecular weights which required lower dosage levels. Their dosage requirement appears to decrease with increasing clay-adsorbing nature as Table I indicates. The weakly clay-adsorbing Polymer B showed a relatively high coating viscosity and long static water retention time. In comparison, the two clay-adsorbing thickeners C and D showed higher thickening efficiency, lower coating viscosity, and shorter static water retention time. The hydropho-bically modified, self-associative thickener D gave the lowest coating liquid viscosity and static water retention time. This is consistent with its strong clay adsorption and low dosage level.

The high shear viscosity of these coatings understandably did not show a simple trend. Polymer A gave a moderately high viscosity. This is characteristic of a less pseudoplastic coating with a relatively large amount of polymer in the liquid phase. The coating containing Polymer B showed a lower high shear viscosity by virtue of its higher pseudoplasticity. Polymer C gave the highest viscosity of all owing to its tendency to hydrogen bond and flocculate clays. In contrast, Polymer D, which is similarly clay-adsorbing, gave a substantially lower viscosity. Previous work has shown that the lower viscosity results from the ease of breaking the hydrophobe to hydrophobe bonds under high shear *(20)*.

We tested the strength of the coatings after subjection to a sudden shear deformation on the rheometer using a stress relaxation method *(21)*. **Figures 8 and 9** show the stress relaxation curves for 60% and 55% solids coatings, respectively. Coatings containing clay adsorbing polymers C and D showed significantly faster after-shear structure recovery indicated by the slower relaxation and a higher after-shear modulus. Their fast structure recovery should benefit coating hold-out during blade coating.

Immobilization solids

We observed the immobilization behavior of the 60% solids coatings on a glass plate using the SGM measurement. This experiment had two purposes. One was to provide baseline data needed to relate on-coater coating gloss to surface moisture. The other was to understand the relative tendency for the coating to form immobilized cake on the coater as **Fig. 10** indicates. All the coatings showed a

11. Immobilization curves for 60% solids coatings

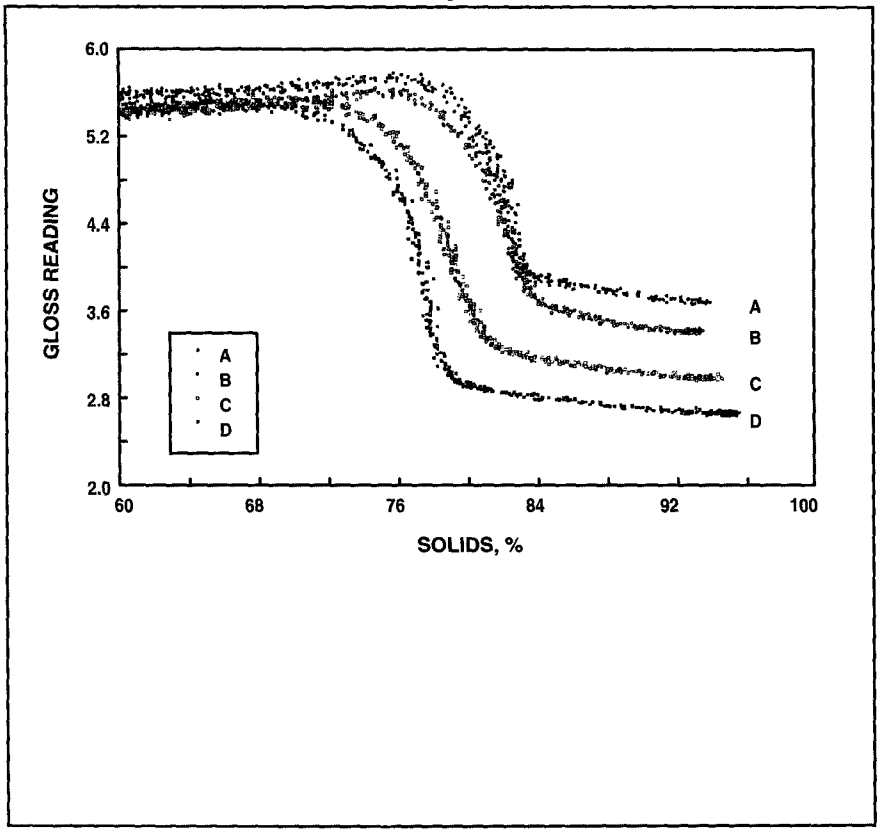

III. Comparison of immobilization solids methods

Polymer	SGM	G&W	Ceramic	VIMS
A	77.2	76.8	74.4	-
B	76.7	75.8	76.0	76.0
C	71.1	70.3	68.0	70.0
D	70.0	69.7	71.7	69.0

similar gloss pattern which is characteristic of coating consolidation. They all begin with a small initial rise in gloss due to leveling of the coating followed by a decline due to consolidation. This eventually levels off to a plateau. The moisture reading of the coating declines always. The rate of decline, however, slows abruptly during the consolidation process. It is not clear now whether this indeed indicates a slowing in moisture loss during consolidation. This phenomenon is under further investigation.

While the coatings all show similar gloss patterns, the time for the coating to reach the GIMS—the solids level at which the gloss begins to decline *(16)*—varies significantly. **Figure 11** gives a comparison of the relative rates of immobilization it shows that differences in the clay–adsorbing nature of the thickeners have a strong impact on the immobilization behavior. The more clay–adsorbing polymers C and D reached the GIMS at relatively low solids values of about 70 and 71%, respectively, as **Table III** indicates. These low GIMS values indicate high levels of solids flocculation caused by thickener and clay association. With so much solids flocculation, the surface water was insufficient to cover the flocs even at these low solids levels. In contrast, the less clay–adsorbing Polymers A and B showed GIMS values that were 6–7% higher. This difference is very substantial considering the large amount of additional water which requires removal for the coating to immobilize.

There is a clear trend of faster immobilization with a more associative thickener. The nonadsorbing Polymer A immobilized so slowly that its GIMS was near that of the thickener–free base coating at a value slightly over 78%. The more adsorbing thickeners also approached the opacity immobilization solids (OIMS) more quickly. At this point, the coating becomes opaque and completely immobilized. The clay–adsorbing thickeners gave a lower gloss after the coating dried. This reflected a higher degree of clay flocculation at the surface of the consolidated coating.

The GIMS values from the SGM method agreed well with those obtained by other methods as Table III shows. The GIMS values from the SGM method were near the values determined by scraping and weighing the coating immediately after onset of the gloss decrease (G&W) method. The G&W method gave slightly lower GIMS values. This could be a result of the higher moisture content of the coating below the surface. We also attempted to measure the GIMS using the unglazed ceramic plate method *(22)*. The results show a trend similar to that with the glass plate methods, although there are some minor discrepancies. The unglazed ceramic plate method was obviously more difficult to practice and was subject to nonuniform coat weight at the surface. It gave a mottled appearance caused by nonuniform plate surface and absorption. The unglazed ceramic plate method also had possible operator errors in reading the gloss value and timing of coating scraping.

The SGM values for the three cellulosic thickeners also agreed well with immobilization solids based on the viscosity measurement of Table III. This viscosity method (VIMS) *(21)* involves laborious measurements of the coating dynamic viscosity at various solids levels. The agreement between GIMS and VIMS values suggests that any test coating at or above the GIMS should have a sharply higher viscosity. This observation is consistent with coatings containing carboxymethylcellulose *(6, 21)*. It also indicates that the much more efficient SGM method is capable of providing all essential in-

12. Gloss curves from CLC tests at (a) 60% solids and 3000 ft 1min, (b) 60% solids and 4000 ft 1 min, (c) 55% and 3000 ft 1 min, and (d) 55% and 4000 ft 1 min.

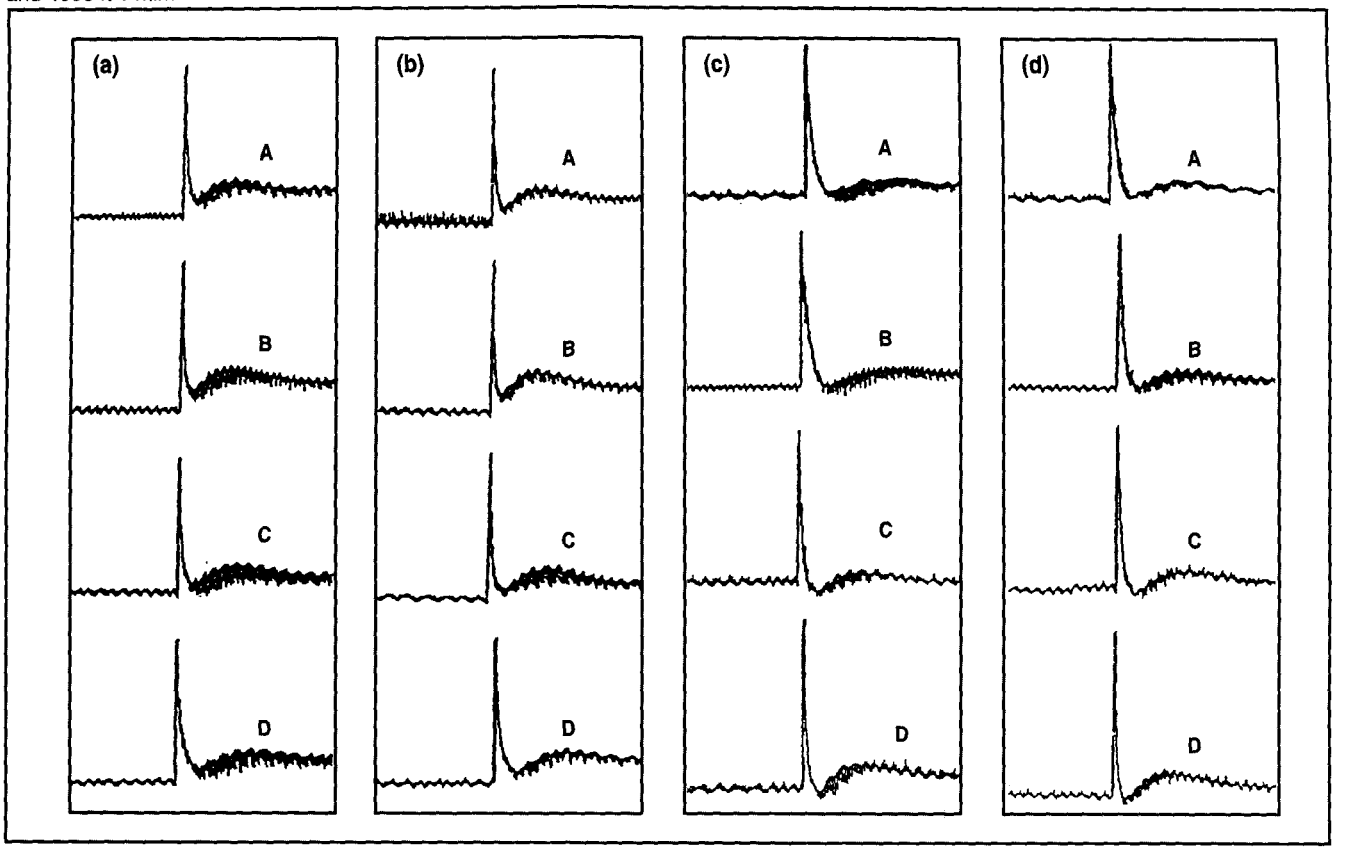

formation about the immobilization process.

Gloss changes on CLC coater

The first series of CLC coater studies involved testing both 55% and 60% solids coatings at 3000 ft/min and 4000 ft/min. The study used a regular post-drying schedule in which drying did not begin until the coated paper had traveled 5 m away from the blade. **Figure 12** illustrates the coating gloss changes observed under such conditions. A sharp rise in gloss occurrs immediately after metering the coating onto the rotating paper. The gloss peaks at a point where the coating covers the entire detecting area. A sharp drop in gloss then follows. This signifies consolidation of the coating due to continued water loss. The gloss reaches a minimum and then begins to rise gradually to a steady value.

What can one learn from such a history of gloss change? We found that virtually all the test coatings were undergoing gloss decay when they traveled to the gloss sensor location. This means that all the test coatings had reached or approached their GIMS by the time the sensor detected them. This was about 0.045 s after blade metering for a speed of 1220 m/min. The sharp drop following the gloss peak should then occur in the coating consolidation process that precedes the OIMS, the decay stage. The rate of this gloss decay should indicate the rate of continued water loss after the blade. Continued capillary migration into the sheet, conceivably through a high solids cake, may cause this water loss. It could also result from a so-called "sponge" effect, i.e., water suction by the basestock recovering from a compressed state under the blade *(10)*.

On the high-speed CLC coater, the gloss decay associated with coating consolidation occurred very quickly. Some of the coatings reached the gloss minimum in a fraction of a second. One expresses the rate of water loss during this stage either in terms of a characteristic decay time (for exponential decay) or the time necessary for the gloss to drop to the minimum value, t_{min}. The gradual rise in gloss after the minimum probably relates to fiber swelling and relaxation *(7)*.

The gloss signal had relatively small noise before coating and larger, equally spaced noise after coating. The baseline noise was largely due to the splicing tape. The after-coating noise was primarily a result of the gloss difference between the coated and uncoated areas on the moving paper. While the noise signals were quite annoying, we were still able to calculate a characteristic decay time, t_d, by fitting the data to an exponential function. **Table IV** gives a summary of the coater conditions and observed gloss decay behavior. Included in the table is the blade run-in. This is the amount of blade travel into the backing roll in mils. There is also the height of the

IV. Gloss decay behavior at 60% and 55% solids

Polymer	Speed, rpm	Blade run-in, mils	Gloss peak height	t_d, ms	t_{min}, s
60% solids					
A	3000	30.0	2.1	245	1.05
A	4000	37.0	2.0	168	0.80
B	3000	24.0	2.1	219	1.05
B	4000	32.0	2.2	189	0.80
C	3000	32.0	1.9	243	1.05
C	4000	40.0	1.9	186	1.12
D	3000	24.0	2.0	333	1.68
D	4000	32.0	2.0	343	1.76
55% solids					
A	3000	24.0	2.0	426	1.89
A	4000	28.0	2.2	318	1.12
B	3000	15.0	2.1	450	1.89
B	4000	22.0	2.1	334	1.60
C	3000	21.5	2.0	215	1.26
C	4000	24.0	2.2	234	1.12
D	3000	11.0	2.2	156	1.26
D	4000	16.0	2.2	165	0.96

V. Gloss decay rates in two CLC tests with long drying delay at 60% solids

Polymer	Speed, rpm	Blade	t_d, ms
A	3000	29.0, 26.5	125, 399
A	4000	38.5, 34.0	96, 223
B	3000	28.0, 24.0	155, 338
B	4000	35.5, 31.0	103, 234
C	3000	31.0, 28.0	195, -
C	4000	39.0, 36.0	104, 312
D	3000	26.0 24.0	127, -
D	4000	33.5, 30.0	107, 380

gloss peak as well as t_d, the characteristic gloss decay time in ms. This is the time for the gloss to drop to 1/e of its peak value. There are also values for t_{min}, the time in s for the gloss to drop to the minimum value.

Gloss decay at varying solids and speeds

We compared the gloss change behavior of the four different coatings on an equal coating weight basis of 5.0 lb/3300 ft² or 7.4 g/m². Recall that the coatings containing Polymers A, B, C, and D in that order had decreasing liquid viscosity, static water retention time, and immobilization solids. If water viscosity were the only factor for water retention, Polymers A through D would have shown increasing gloss decay rates and decreasing gloss peak values. Such a simple trend did not occur. At 60% solids, Polymer D, which had the shortest water retention time, showed the slowest gloss decay according to the t_d and t_{min} values in Table IV. Its gloss retention character was more noticeable at 4000 ft/min. It had a gloss peak value near that of Polymer A at 4000 ft/min. This should also be a sign of good water retention, since Polymer D during the consolidation stage would have a much lower gloss than Polymer A at the same solids. An earlier pilot coater trial from a similar associative cellulosic polymer also showed surprisingly good water retention for Polymer D *(19)*.

The outstanding gloss retention of Polymer D may be a result of its superior cake formation capability. The much lower immobilization solids and fast-recovering coating structure effected by the strongly associative Polymer D should facilitate the cake formation process. This cake formation effect should be more pronounced at higher speeds. Here a shorter, larger pressure pulse associated with the higher speed may cause substantially higher pressure migration, if there is no cake barrier formation. Table IV also shows that the coatings containing Polymer D could operate at a relatively low blade pressure as indicated by the small amount of blade displacement into the backing roll. The low blade pressure should also benefit water retention, since it means there is a relatively small driving force for pressure migration. The low blade pressure is consistent with its relatively low viscosity. This corresponds to the ease in breaking hydrophobe to hydrophobe associations. Polymer D therefore appears to be unique in giving coatings that are highly structured, quickly immobilized, and easily metered.

Polymer C, the other clay-adsorbing material, showed a satisfactory but somewhat lower gloss retention at 60% solids. At this relatively high solids level, it probably had caused too much solids flocculation by virtue of strong hydrogen bonding with clays. This resulted in higher blade pressures which could have caused increased pressure-driven water loss.

The gloss retention of Polymer D was much poorer at the lower 55% solids. At this low solids, there would have to be a much larger amount of water lost before solids immobilization and cake formation took place. Consequently, the cake formation effect appears to be largely diminished, and water retention is more dependent on the liquid phase viscosity.

One should note here that the gloss decay behavior in this series of studies was under the influence of post-dry-

ing. While there was a short delay in IR drying, drying began in the middle of the gloss decay stage. This complication should not have changed the relative rate of gloss decay cited above, since there was no reason for the clay-adsorbing polymers to dry slower under IR irradiation than the non-adsorbing polymers which gave much higher water viscosities. This was indeed the case according to results from two other series of CLC tests in which post-drying began long after full consolidation of the coating. **Table V** gives the relative gloss decay rates and blade pressures for these two tests at 60% solids. The data is from two separate CLC tests using two different sources of basestocks and clays. The second trial used a modified sensor head located closer to the blade. It was about 1.5 ft away instead of 3 ft. Some of the data for t_d is missing because the computer only captured part of the decay curve. There was therefore insufficient data for proper fitting. While absolute decay times varied, the relative rates followed the same trend discussed above. The clay-adsorbing polymers and Polymer D in particular again showed superior gloss retention at this high solids level.

The differences in absolute decay time were due to the changes in testing conditions. The shortened time for the coating to reach the detector resulted in higher gloss peak values and longer gloss decay times.

Water loss in low-speed tests

We have conducted a short test on the slower bench-top coater at a speed of about 40 ft/min. The gloss decay time in this study was considerably longer as Fig. 3 indicates. With 60% solids coatings, it took over 10 s for the gloss to reach a minimum in contrast to a fraction of a second for high-speed CLC coater tests. At 60% solids, Polymer D showed faster decay than Polymer A in this test. This contradicted the CLC test observation. The discrepancy is probably the result of an unrealistically low blade pressure associated with the low speed. Under bench-top conditions, cake formation is unlikely to occur to a significant degree. In addition, capillary migration and vapor sorption are likely to control water loss *(3)*.

The widely practiced test for water retention time obviously suffers from the same deficiency. In this test, water loss occurs under virtually no pressure over a typical time of over 10 s. The lack of a pressure pulse leads to relatively slow water migration from the coating "fluid" to the paper by capillary forces. Cake formation seems unlikely until after immobilization of much of the coating. As a result, this type of test tends to favor less associative thickeners which generally give a higher coating water viscosity. Conclusions based on the test can therefore be misleading in situations where the cake formation mechanism is important.

VI. Optical and printing properties of calendered paper at 5.0 ± 0.1 lb/3300 ft²

	Polymer			
	A	*B*	*C*	*D*
60% solids, 3000 rpm:				
Gloss, %	50.6	50.4	45.9	51.2
Opacity, %	79.1	79.1	78.8	79.5
Brightness, %	66.6	66.8	67.3	66.8
Helio, mm @ 75 kgf	70	74	79	77
PPSs (μ) @ 10 kgf/cm²	1.39	1.34	1.32	1.29
60% solids, 4000 rpm:				
Gloss, %	50.8	49.0	45.1	50.5
Opacity, %	79.0	79.0	79.0	80.1
Brightness, %	66.7	66.8	67.2	67.0
Helio, mm @ 75 kgf	71	67	73	80
PPS (μ) @ 10 kgf/cm²	1.38	1.39	1.33	1.34
55% solids, 3000 rpm:				
Gloss, %	47.2	49.3	43.5	46.5
Opacity, %	79.1	79.4	78.9	78.7
Brightness, %	66.5	67.0	67.3	66.7
Helio, mm @ 75 kgf	64	67	74	77
PPS (μ) @ 10 kgf/cm²	1.49	1.43	1.43	1.35
55% solids, 4000 rpm:				
Gloss, %	46.5	48.0	46.0	46.0
Opacity, %	79.0	78.8	79.8	78.5
Brightness, %	67.0	66.8	67.4	66.7
Helio, mm @ 75 kgf	63	63	76	74
PPS (μ) @ 10 kgf/cm²	1.47	1.45	1.38	1.38

Optical and printing properties

We measured optical and rotogravure printing properties of the coated paper samples in an attempt to relate the water loss and immobilization properties to the coated paper quality. **Table VI** summarizes the results for calendered papers at varying solids and speeds. At 60% solids, the most associative material, Polymer D, showed significantly better opacity, smoothness, and Helio missing dots than the non-associative polymers. The superior coated paper quality coincides with its good on-coater water retention performance at this solids by virtue of cake formation. Cake formation also appears to contribute to coating holdout as well as surface coverage and smoothness *(9, 23)*.

Polymer C also showed good smoothness and rotogravure printability by virtue of its strong affinity to clays. Its strong affinity toward paper indicated in Table I, which should ben-

efit solids retention and cake formation, could have also contributed to good surface coverage. Its gloss value, however, was significantly lower than Polymer D at this high solids despite its good smoothness. Other investigators have reported this relatively low gloss in high solids clay coatings *(20, 24)*. A possible explanation may exist in terms of strong clay flocculation. The floc structure involves primarily hydrogen bonding and is relatively difficult to break under high shear. At 60% solids, the number of clay/thickener/clay bonds can be so large—there can be 10^{15} clay-bonded polymer molecules under a typical production blade—that a substantial portion of them are not mechanically broken under the blade. The coating surface after splitting from the blade can therefore consist of many clay flocs. These flocs can cause a considerable increase in the micro-roughness of the coating surface leading to lower gloss. This over-flocculation related problem should be less severe at a lower solids.

An explanation of the relatively high gloss values for Polymer D at 60% may also result from its associative behavior. Unlike Polymer C, which causes clay flocs only through hydrogen bonding, Polymer D can also undergo hydrophobe to hydrophobe associations. These involve London and van der Waals forces that are several times weaker than hydrogen bonds. They break much more easily under the blade. Consequently, the coating surface after the blade should have much fewer, smaller flocs and lower micro-roughness. This lower micro-roughness together with a low macro-roughness due to good fiber coverage gives good gloss.

The two clay-adsorbing polymers still showed good smoothness and rotogravure printability at 55%. The overall performance of Polymer D at this low solids, however, deteriorated appreciably coinciding with its relatively poor water retention. This indicates again that the benefit of cake formation has diminished appreciably at low solids.

Summary

The results of this work suggest that the noncontact reflection detector should be a useful tool for the study of coating water loss and immobilization under high-speed conditions. The four thickeners used in this study, although not necessarily representing the best commercial practice, illustrate the significance of thickener to pigment interactions in water retention, immobilization behavior, and finished paper quality. While this work focuses on the effect of clay and thickener interactions, the use of the noncontact reflection detector has no definite limit to such studies. We would expect the work to be useful in studying other factors that may influence water retention such as variations in the basestock, sizing, temperature, blade angle, pigment, geometry, and size distribution. With minor modifications such as installing additional sensing heads, this technique may also apply to pilot or production coaters.

The results of our study lead to the following conclusions:

- A computer-interfaced noncontact gloss detector with a CLC laboratory coater can study coating dewatering and immobilization under short pressure pulses typically experienced on high-speed, short-dwell-type blade coaters.
- Gloss decay data from the CLC coater indicates that water retention on a short-dwell-type coater depends not only on the coating water viscosity but also the capability of the coating to form a high solids cake barrier at the coating to paper interface. For clay-based rotogravure coatings, relative dewatering rates from low speed or static tests do not correlate with dewatering rates from the CLC coater at high speeds.
- Interactions between the water soluble polymeric thickener and clays strongly influence coating water retention. For clay-adsorbing cellulosic thickeners which tend to cause more structure building and faster immobilization, the cake formation mechanism appears to play a major role in limiting water loss.
- Nonionic clay-adsorbing thickeners tend to give better opacity, smoothness, and rotogravure printability than thickeners with low clay affinity. These properties relate to the high degree of solids flocculation and low immobilization solids from clay and thickener association. The superior finished paper properties of clay-adsorbing thickeners were accompanied by good water retention under conditions that favor cake formation.
- The noncontact gloss detector with a near-IR detector can simultaneously measure coating gloss and moisture over the entire consolidation process. The simultaneous gloss and moisture measurement offer an efficient and reproducible technique to study the coating consolidation process and immobilization solids. TJ

Literature cited

1. Clark, N. O., Windle, W., and Beazley, K. M., *Tappi* 52(11): 2191(1969).
2. Windle, W., Beazley, K. M., and Climpson, M., *Tappi* 53(12): 2232(1970).
3. Eklund, D. E. and Salminen, P., *Tappi J.* 69(9): 116(1986).
4. Salminen, P. J., *TAPPI 1988 Coating Conference Proceedings*, TAPPI PRESS, Atlanta, p. 133.
5. Sandas, P. E., Salminen, P. J., and Eklund, D., *TAPPI 1989 Coating Conference Proceedings*, TAPPI PRESS, Atlanta, p. 37.
6. Herbet, A. J., Gautam, N., and Whalen-Shaw, M. J., *TAPPI 1990 Coating Conference Proceedings*, TAPPI PRESS, Atlanta, p. 387.
7. Sakano, M. and Shigetomi, K., Jap. *TAPPI* 44(11): 62(1990).
8. Jones, S. W. and Hetherington, L. E., *Tappi J.* 63(4): 137(1980).
9. Baumeister, M. and Kraft, K., *Tappi* 64(1): 85(1981).
10. Fujiwara, H., Fujisaki, N., Shimizu, I., *et al.*, *Tappi J.* 72(5): 91(1989).
11. Fujiwara, H., Fujisaki, N., and Kaga, C., *TAPPI 1991 Coating Conference Proceedings*, TAPPI PRESS, Atlanta, p. 179.
12. Herbet, A. J., Review Methods to Measure Coating Immobilization Solids and Associated Coating Dehydration Rates, TAPPI PRESS, Atlanta, 1988.

13. Chen, K.S.A. and Scriven, L. E., *TAPPI 1989 Coating Conference Proceedings,* TAPPI PRESS, Atlanta, p. 93.
14. Gane, P.A.C., Watters, P., and McGenity, P. M., TAPPI 1992 Coating Conference Proceedings, TAPPI PRESS, Atlanta, p. 117.
15. Engström, G., Norrdahl, P., and Ström, G., *TAPPI 1987 Coating Conference Proceedings,* TAPPI PRESS, Atlanta, p. 35.
16. Lepoutre, P., Coating Structure: A Review, TAPPI PRESS, Atlanta, 1988.
17. Washburn, E.W., *The Phys. Rev.* 17(13): 273(1921).
18. Lafaye, J. F., Gervason, G., Maume, J. P., *et al.*, TAPPI 1987 Coating Conference, TAPPI PRESS, Atlanta, p. 107.
19. Lonkila, S., "Paksuntajan voikutus päällyslyspastan vesiretentioon ja rcologiaan", M.S. thesis, Oulu University, Finland, 1989.
20. Young, T. S. and Fu, E., *Tappi J.* 74(4): 197(1991).
21. Young, T. S. and Fu, E., *TAPPI 1991 Coating Conference Proceedings,* TAPPI PRESS, Atlanta, p. 61.
22. Beck, U., Goossens, J.W.S., Rahlwes, D., *et al., TAPPI 1983 Coating Conference Proceedings,* TAPPI PRESS, Atlanta, p. 47.
23. Weigl, J. and Baumgarten, H. L., *Dtsch. Papierwirtsch.* 2:52(1984).
24. Barber, E. J., *Tappi* 56(1): 52(1973).

The authors thank the following colleagues who have made invaluable contributions to this work: Gregory Bramwell and James Kirwin, for their assistance throughout the laboratory coating studies and CLC tests; Steve Kittleson, Edward Morawski, and Michele Watson for conducting the CLC and paper properties tests; Bernard Matyniak for rebuilding the gloss detector; Robert Grasso, George Groseclose and Wayne Gibbons for assistance and consultation in computer analysis; and Linda Kline for preparation of the manuscript.

Received for review Dec. 9, 1992.

Accepted Jan. 29, 1993.

Presented at the TAPPI 1993 Coating Conference.